

Multiple Hydrogen-Bonded Complexes Based on 2-Ureido-4[1H]-pyrimidinone: A Theoretical Study

Hao Sun,^{†,‡} Hui Hui Lee,^{§,||} Idriss Blakey,[§] Bronwin Dargaville,[§] Traian V. Chirila,^{§,||,⊥,‡}
Andrew K. Whittaker,^{§,||,▽} and Sean C. Smith^{*,‡}

[†]Faculty of Chemistry, Institute of Functional Material Chemistry, Northeast Normal University, 130024 Changchun, Jilin, People's Republic of China

[‡]Centre for Computational Molecular Science, Australian Institute for Bioengineering, Nanotechnology, The University of Queensland, St. Lucia, Queensland 4072, Brisbane, Australia

[§]Australian Institute for Bioengineering and Nanotechnology, The University of Queensland, St. Lucia, Queensland 4072, Australia

^{||}Queensland Eye Institute, South Brisbane, Queensland 4101, Australia

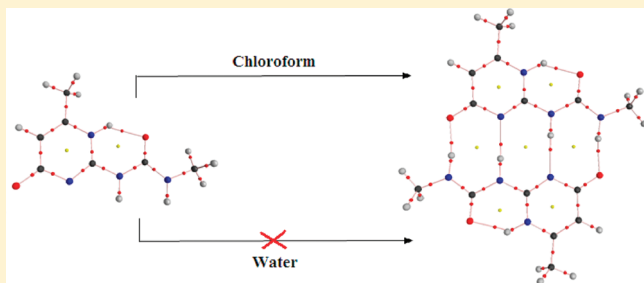
[⊥]Discipline of Chemistry, Faculty of Science and Technology, Queensland University of Technology, Brisbane, Queensland 4001, Australia

[‡]Faculty of Health Sciences, The University of Queensland, Herston, Queensland 4006, Australia

[▽]Centre for Advanced Imaging, The University of Queensland, St. Lucia, Queensland 4072, Australia

S Supporting Information

ABSTRACT: In the present work, the electronic structures and properties of a series of 2-ureido-4[1H]-pyrimidinone (UPy)-based monomers and dimers in various environments (vacuum, chloroform, and water) are studied by density functional theoretical methods. Most dimers prefer to form a DDAA-AADD (D, H-bond donor; A, H-bond acceptor) array in both vacuum and solvents. Topological analysis proved that intramolecular and intermolecular hydrogen bonds coexist in the dimers. Frequency and NBO calculations show that all the hydrogen bonds exhibit an obvious red shift in their stretching vibrational frequencies. Larger substituents at position 6 of the pyrimidinone ring with stronger electron-donating ability favor the total binding energy and free energy of dimerization. Calculations on the solvent effect show that dimerization is discouraged by the stronger polarity of the solvent. Further computations show that *Dimer-1* may be formed in chloroform, but water molecules may interact with the donor or acceptor sites and hence disrupt the hydrogen bonds of *Dimer-1*.



INTRODUCTION

In recent years, the multiple-point hydrogen-bonding motifs have been used rather extensively to generate supramolecular polymer networks based on reversible, noncovalent interactions.^{1–14} Such interactions must be able to hold together the constitutive parts of a supramolecular polymer and to ensure a degree of “polymerization” sufficiently high to induce material properties that can be maintained in ambient conditions and can be described in light of the tenets of polymer physics. Due to the directionality and strength (when multiple bonds act cooperatively) of the hydrogen bond, its formation has been advocated as an effective tool to promote self-assembling processes leading to supramolecular polymers. The first reports on hydrogen-bonded supramolecular systems involving polymers came from Lehn's group¹⁵ and from Kato's and Fréchet's¹⁶ laboratories. Ever since, various research teams made considerable efforts to synthesize molecules where several hydrogen-bonding modules

were built into arrays of donor (D) and acceptor (A) functionalities.

In principle, to fulfill their role in the formation of supramolecular polymers, the motifs with hydrogen-bonding arrays should be attached to suitable progenitors either as telechelic units or as side chains. Although arrays from two to eight D and A functionalities in a single structural motif have been reported, only a few such motifs were actually used to generate supramolecular polymers due to difficulties in further functionalizing them. Besides, classic monomers containing multiple hydrogen-bonding motifs have notoriously low solubility in the solvents that are commonly used as polymerization media.

Received: June 29, 2011

Revised: August 3, 2011

Published: August 11, 2011

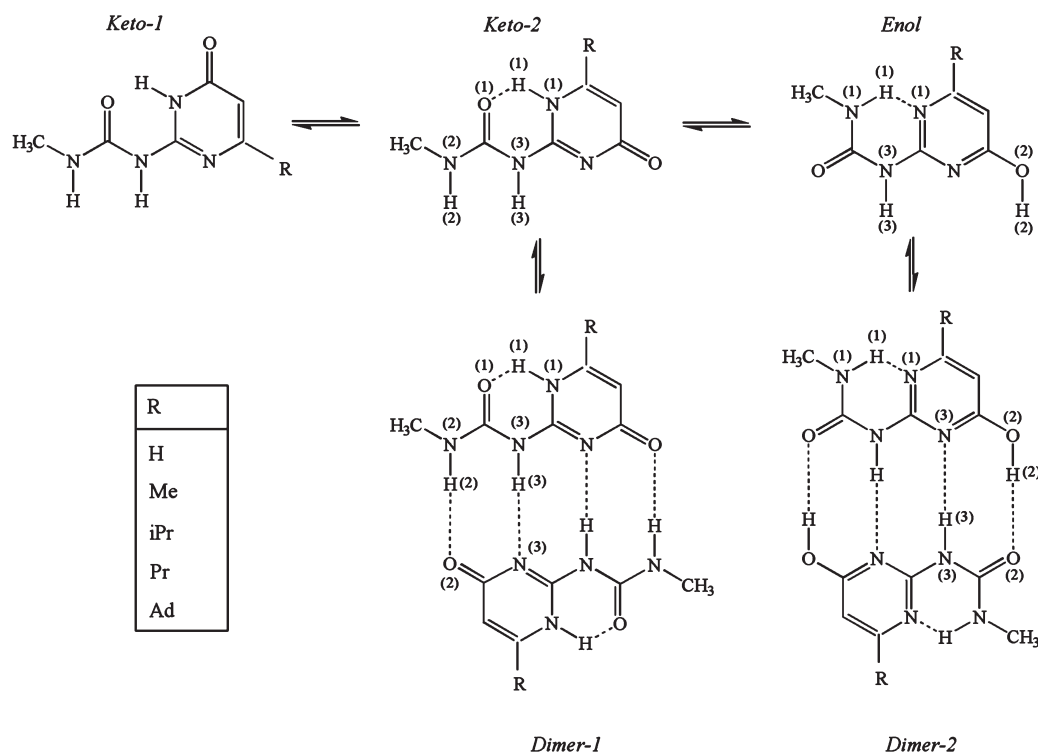


Figure 1. Tautomer and monomer–dimer equilibria in the UPy system.

When the hydrogen-bonding arrays interact, they can generate aggregates. The latter can be based on homodimers, when two identical motifs interact in such a way that the arrangement of the interacting functionalities (D, A) is self-complementary, or on heterodimers, when two different motifs interact in a complementary arrangement of their functionalities.

The quadruple hydrogen-bonding arrays have been particularly successful in the formation of supramolecular aggregates, including supramolecular polymers. Of the six possible dimeric quadruple hydrogen-bonding arrays (ADAD-DADA, AADD-DDAA, ADDA-DAAD, ADAA-DADD, AAAD-DDDA, and AAAA-DDDD),¹⁷ only the first three have been explored (ADAD-DADA,¹⁸ AADD-DDAA,^{19–23} ADDA-DAAD^{24,25}). Lünig's group reported ADAA-DADD²⁶ and AAAA-DDDD²⁷ heterodimers, but the values of the association constant (K_a) measured for these complexes were extremely low ($K_a \leq 590 \text{ M}^{-1}$ and, respectively, $K_a = 525 \text{ M}^{-1}$, both in chloroform- d_1), indicating that the existing intramolecular hydrogen bonding favors conformers/tautomers where the intermolecular complementarity was prevented. However, Leigh et al.²⁸ reported recently a heterodimeric AAAA-DDDD array that showed excellent stability ($K_a > 3 \times 10^{12} \text{ M}^{-1}$ in dichloromethane, $K_a = 3.4 \times 10^5 \text{ M}^{-1}$ in 10% DMSO- d_6 /90% chloroform- d_1), which can be a result of favorable secondary electrostatics. Indeed, the sequence of D and A functionalities in an array is important due to the induced secondary electrostatic interactions, an effect demonstrated for the first time by Jorgensen in triply hydrogen-bonded aggregates.²⁹ Accordingly, the strength of an individual hydrogen bond is affected by the adjacent D and A atoms. Thus, an acceptor will be less attracted to its donor partner if the latter is located next to another acceptor. If a donor is next to another donor, the attraction between the former and its acceptor partner will be reinforced. Consequently, in an AAAA-DDDD array all

secondary interactions reinforce the attraction between main D and A atoms, and—provided that the conformation of the motif's tautomer is adequate—such an array would lead to the most stable hydrogen-bonded aggregates. Leigh's work²⁸ confirmed this prediction.

To date, the array used most extensively (and successfully) to generate supramolecular polymer networks has been the homodimeric AADD-DDAA array developed by Meijer's group,^{19–21,30–35} on the basis of 6-substituted 2-ureido-4[1H]-pyrimidinones (henceforth, UPy). The UPy motifs can be conveniently synthesized in gram-scale amounts and are relatively easy to modify. Three different tautomers of 2-ureido-4[1H]-pyrimidinone are present in solution,^{20,32} as shown in Figure 1. The tautomeric equilibrium constants (K_{taut}) are concentration-dependent and influenced by the polarity of solvent. The *o*-quinonoid form *Keto-1*, a 4[3H]-pyrimidinone (or 6[1H]-pyrimidinone), can be predominant in certain media,³⁰ as it happens also in the case of the parent compound 2-amino-4-pyrimidinone (isocytosine);^{36,37} however, this tautomer cannot dimerize through four hydrogen bonds. The *p*-quinonoid form *Keto-2*, a 4[1H]-pyrimidinone, and the phenolic form *Enol*, a 4[1H]-pyrimidinol, have a strong tendency to dimerize via the homodimeric quadruple hydrogen-bonding arrays AADD-DDAA and DADA-ADAD, respectively. Intramolecular hydrogen bonding in these tautomers can further stabilize the dimers. The four cooperative hydrogen bonds responsible for dimer formation lead to stable complexes in nonpolar solvents, where generally the tautomer *Keto-2* is favored. However, the *Enol* form prevails in the UPy motifs possessing electron-withdrawing substituents (e.g., *p*-nitrophenyl, trifluoromethyl) at the 6-position.²⁰

Supramolecular polymers based on UPy hydrogen-bonding motifs are materials displaying many new, potentially useful properties resulting from a combination of the properties of

conventional polymers used as building blocks with the reversibility features generated by the directional and reversible multiple hydrogen bonds. Such properties can be further diversified by controlling the energetic aspects of bonding through a rational modification of the UPy motifs. The formation of UPy-based dimers in polar solvents, including water, remains an open challenge. In spite of a vast experimental literature, a systematic theoretical study has yet to be reported, particularly regarding the effect of the substituents at 6-position of the pyrimidinone ring, and the correlation of this effect to the changes in the nature and concentration of solvent.

In the present study, we investigated the nature of hydrogen bonds and interaction energies of UPy-based dimers, including electronic properties, interactions between donating and accepting orbitals of hydrogen bonds, and the effect of the structure of 6-substituents and solvents on dimer formation. Our computations will give a comprehensive investigation into the UPy dimerization in various environments and provide theoretical direction for obtaining stable dimers based on UPy in water.

COMPUTATIONAL METHODS

There have been numerous reports to demonstrate that density functional theoretical (DFT) methods can describe weakly interacting systems efficiently,^{38–43} although it takes less comprehensive electron correlations into account than the MP2 method. B3LYP^{44,45} was considered as an appropriate method to calculate multiple hydrogen bonded complexes.^{38–42} Considering the balance of accuracy and the computational economy, the 6-31G(d) basis set was used to optimize the structures of all the possible monomers and dimers in a vacuum and in solvents. To test the applicability of the B3LYP/6-31G(d) model to systems studied here, the B3LYP/6-31G(d) geometry of the UPy dimer has been compared with those obtained at higher level B3LYP/6-311+G(d,p)³⁴ for available structures before optimizations for all the systems studied herein. The geometric differences between the two computational levels are negligible with the largest deviation 0.8% (Figure 1S of the Supporting Information), indicating that the B3LYP/6-31G(d) optimizations can provide credible structures. The optimized structures were confirmed to be minima by frequency analysis. On the basis of the optimized structure, further single point energies and natural bond orbitals (NBO) were calculated at the B3LYP/6-311++G(2d,2p) level. Because our experiments showed the states of the complexes we studied were different in chloroform and water, the influence of solvent was included for optimization and single point energy computations using polarizable continuum models (PCM),^{46,47} in which the cavity was created via a series of overlapping spheres. Optimization, frequency, and NBO computations were carried out using Gaussian 09.⁴⁸ To gain a more comprehensive understanding of the hydrogen bonding in this system, topological properties of electron densities in the UPy-6-Me monomer and dimer were calculated at the B3LYP/6-311++G(2d,2p) by G09 combined with AIM2000⁴⁹ code.

An important problem for predicting weak interactions is basis set superposition error (BSSE). To obtain more accurate binding energies, BSSE was corrected for all calculations by using the widely reported counterpoise (CP) method^{50,51} based on the optimized geometries. It should be noted that the CP method is not compatible with the PCM model. Therefore, BSSEs for dimers in solvents were calculated without involving PCM model based on their structures in the corresponding solvents. The energies in

the paper are the results at the B3LYP/6-311++G(2d,2p)//B3LYP/6-31G(d) level unless otherwise stated.

RESULTS AND DISCUSSION

Structural Features of Monomers and Dimers. Table 1 and Table 1S (Supporting Information) list the geometric parameters and vibrational stretching frequencies of hydrogen bonds for all the monomers and dimers shown in Figure 1. From the energies in Table 2, *Dimer-1* is more stable than *Dimer-2* in chloroform and water. (to be discussed in detail further) Therefore, our emphasis in the following discussion focuses primarily on *Dimer-1*.

Under the various conditions (vacuum, chloroform and water), our data from Table 1S and Figure 2S (Supporting Information) showed that all three N–H bonds are elongated when *Keto-2* generates *Dimer-1*. The largest increase of all N–H bond lengths was observed for vacuum. For the situation in solvent, the increase of N(1)–H(1) bond is larger in chloroform than in water, whereas no significant change was observed for different solvents for N(2)–H(2) and N(3)–H(3) bonds. In each environment, the N(2)–H(2) bond is elongated more as compared to the N(3)–H(3), whereas the N(1)–H(1) bond has the smallest increase. Table 1S and Figure 3S (Supporting Information) show that the distances of H(1)---O(1) in *Dimer-1* vary from 1.7380 to 1.7441 Å in a vacuum, from 1.7610 to 1.7666 Å in chloroform and from 1.7726 to 1.7775 Å in water. Such bond distances are typical of hydrogen bond length,⁵² and further confirmation of H-bonding will be gained from AIM and NBO analysis below (in the further sections). The distances between O(1) and H(1) decreased when dimers formed. The extent of contraction of intramolecular H-bond decreased when going from vacuum to chloroform and water. N(3)–H(3)---N(3) bonds are the longest among all three hydrogen bonds in the various environments studied. All N(1)–H(1)---O(1) bond lengths are approximately the same as the corresponding N(2)–H(2)---O(2) bonds, with the exception of the N(1)–H(1)---O(1) bond length in a vacuum. For example, intermolecular hydrogen bonds N(2)–H(2)---O(2) and N(3)–H(3)---N(3) of UPy-6-Me dimer are 1.7630 and 1.9742 Å in a vacuum, 1.7660 and 1.9928 Å in chloroform, and 1.7668 and 2.0020 Å in water, respectively.

Regarding the effect of the substitution group, dimers with the adamantyl group have the shortest hydrogen bonds, although not all the hydrogen bonds exhibit linear shortening in the order of increasing size of substitution groups.

Table 1 shows that when compared to the monomer *Keto-1*, all dimers have considerably reduced stretching frequencies for the three N(O)–H bonds involved in hydrogen bonding, indicating an obvious red shift of their IR spectrum. N(2)–H(2) exhibits the largest decrease in amplitude, followed by N(3)–H(3) and finally N(1)–H(1). Taking UPy-6-Me as an example, the $\Delta\nu$ values of N(1)–H(1), N(2)–H(2), and N(3)–H(3) are -180.95 cm^{-1} (-117.22 cm^{-1} , -90.70 cm^{-1}), -350.25 cm^{-1} (-361.09 cm^{-1} , -368.90 cm^{-1}), and -324.65 cm^{-1} (-339.53 cm^{-1} , -340.28 cm^{-1}), respectively (values in parentheses correspond to those in chloroform and in water). The larger the substituent, the larger the red shifts of N(2)–H(2) and N(3)–H(3) bonds exhibited, whereas N(1)–H(1) follows an opposite trend. It can be deduced that redistribution of charge caused by the substituents has a different effect on intramolecular and intermolecular hydrogen bonds.

Table 1. Vibrational Stretching Frequencies (cm^{-1}) for N(1)–H(1), N(2)/O(2)–H(2), and N(3)–H(3) Bonds in *Keto-2* and *Dimer-1*^a

R		vacuum			chloroform			water		
		N(1)–H(1)	N(2)/O(2)–H(2)	N(3)–H(3)	N(1)–H(1)	N(2)/O(2)–H(2)	N(3)–H(3)	N(1)–H(1)	N(2)/O(2)–H(2)	N(3)–H(3)
H	<i>Keto-2</i>	3460 (379)	3628 (41)	3602 (29)	3435 (552)	3624 (85)	3602 (40)	3425 (630)	3630 (103)	3602 (56)
	<i>Dimer-1</i>	3272	3286	3286	3315	3272	3272	3334	3270	3270
		(1297)	(4173)	(4173)	(1426)	(5266)	(5266)	(1539)	(5045)	(5045)
Me	<i>Keto-2</i>	3453 (342)	3628 (41)	3602 (29)	3425 (512)	3626 (83)	3604 (42)	3413 (594)	3631 (105)	3603 (57)
	<i>Dimer-1</i>	3277	3277	3277	3308	3265	3265	3322	3262	3262
		(1380)	(997)	(3426)	(1346)	(5670)	(5670)	(1496)	(5715)	(5715)
Pr	<i>Keto-2</i>	3454 (317)	3628 (42)	3602 (29)	3423 (498)	3629 (68)	3606 (60)	3409 (594)	3631 (89)	3605 (71)
	<i>Dimer-1</i>	3276	3273	3273	3306	3261	3261	3320	3259	3259
		(1007)	(5136)	(5136)	(1236)	(6079)	(6079)	(1477)	(6095)	(6095)
iPr	<i>Keto-2</i>	3455 (317)	3627 (82)	3602 (29)	3421 (494)	3628 (72)	3603 (54)	3407 (585)	3630 (92)	3601 (68)
	<i>Dimer-1</i>	3277	3272	3272	3308	3261	3261	3321	3258	3258
		(965)	(5119)	(5119)	(1272)	(4467)	(4467)	(1450)	(4876)	(4876)
Ad	<i>Keto-2</i>	3463 (283)	3627 (44)	3602 (30)	3430 (459)	3625 (81)	3605 (49)	3415 (565)	3628 (106)	3603 (59)
	<i>Dimer-1</i>	3291	3270	3270	3315	3258	3258	3330	3257	3257
		(822)	(5175)	(5175)	(1183)	(6460)	(6460)	(1388)	(6442)	(6442)
		[−172]	[−357]	[−332]	[−115]	[−366]	[−347]	[−85]	[−371]	[−346]

^a Note: Values in parentheses are the corresponding IR densities (km/mol). The decrease of the stretching frequencies is listed in square brackets.

Energy and Solvent Effects. *Energy of Monomers and Dimers.* Table 2 lists BSSE and correction of zero-point energy (ZPE) and energies of all monomers and dimers as well as the binding energies and free energies for dimerization of *Dimer-1*. The stability of monomers is in the order *Enol* > *Keto-1* > *Keto-2* in a vacuum, *Keto-1* > *Enol* > *Keto-2* in chloroform, and *Keto-1* > *Keto-2* > *Enol* in water. *Dimer-1* is more stable than *Dimer-2* in the various environments, with the exception of the dimers of UPy-6-H, UPy-6-Me, and UPy-6-iPr in a vacuum. Therefore, it can be seen that the polarization of the surrounding environment has a significant influence on the stability of both monomers and dimers. For example, the energies of *Keto-1* forms of UPy-6-Me, are 6.28, 3.89, and 2.76 kcal/mol lower than of the corresponding *Keto-2* forms in a vacuum, chloroform, and water, respectively. The energy of the *Enol* form is 7.47 and 1.88 kcal/mol lower than those of *Keto-2* in a vacuum and chloroform, respectively, but is 1.19 kcal/mol higher in water. Therefore, *Keto-1* is the most favorable form of monomer in solvents. *Dimer-1* of UPy-6-Me has the energy by 1.51 and 2.82 kcal/mol lower than *Dimer-2* in solvents, whereas the energy of *Dimer-2* is 0.44 kcal/mol lower than that of *Dimer-1* in a vacuum. That is to say, from the viewpoint of energy, these UPy-based monomers tend to favor the DDAA-AAADD binding array in chloroform and water, whereas they favor the DADA-ADAD binding array in a vacuum. These conclusions agree with available experimental reports that the DDAA form of UPy dimer has a larger dimerization constant in chloroform.^{20,30,32}

Interaction Energy of Dimers and Substituent Effects. From Table 2, BSSE values do not vary with the structure of the substitution group and solvent. However, large basis sets can reduce BSSE efficiently, and it can be neglected at the

B3LYP/6-311++G(2d,2p) level. To determine the hydrogen bonding strength, binding energy was calculated according to the eq 1:

$$E_b = E_{\text{dimer}} - 2E_{\text{monomer}} \quad (1)$$

From Table 2, larger substituents with a stronger electron-donating ability, leads to a higher binding energy of *Dimer-1*. Figure 2 depicts the plot of binding energies of *Dimer-1* in various environments. Here, the effect of the substituent on binding energy is not distinct. For example, the binding energy of UPy-6-H in chloroform is −23.45 kcal/mol, only 0.86 kcal/mol lower than that of UPy-6-Ad dimer (−24.31 kcal/mol). As listed in Table 2, the binding energies of *Dimer-1* in various environments are in the range from −38.26 to −39.66 kcal/mol in a vacuum, −23.45 to −24.31 kcal/mol in chloroform, and −16.58 to −17.37 kcal/mol in water. Obviously, the nature of solvent has a considerable effect on binding energies, indicating that the choice of solvent is crucial for dimerization to take place. Taking *Dimer-1* of UPy-6-Me as an example, the binding energies are 23.88 kcal/mol in chloroform and 17.07 kcal/mol in water, indicating that weakly polar solvents favor the formation of stable DDAA-AAADD dimers. Although the binding energy of *Dimer-1* in water is much weaker than in chloroform, it is still in the range of strong hydrogen bonding.⁵²

Of course, considerations based on binding energy alone do not account for the substantial loss of entropy that occurs upon dimer formation, which impacts significantly the overall free energy change. This is due to the transformation of rotational entropy in the separated monomers into vibrational entropy of the intermonomer “rocking” motions within the dimers. To get

Table 2. ZPE, BSSE, Energies of Monomers and Dimers, and Binding Energies and Free Energies for Dimerization^a

R	vacuum						chloroform						water					
	^a ZPE	^a BSSE	^a E _b	^b BSSE	^b E _b	^b ΔG	^a ZPE	^a BSSE	^a E _b	^b BSSE	^b E _b	^b ΔG	^a ZPE	^a BSSE	^a E _b	^b BSSE	^b E _b	^b ΔG
H																		
Keto-1	97.08				−602.9996		97.08				−603.0141		97.01				−603.0203	
Keto-2	96.89				−602.9898		97.01				−603.0083		96.89				−603.0168	
Dimer-1	196.03	6.69	−39.75	0.89	−1206.0406	−38.26	195.59	6.67	−26.40	0.88	−1206.0539	−23.45	195.41	6.67	−20.63	0.89	−1206.0600	−16.58
Enol	97.33				−603.0011		97.01				−603.0102		96.89				−603.0145	2.05
Dimer-2	195.85	6.91	−25.28	0.97	−1206.0417	−24.84	195.28	6.90	−20.08	0.97	−1206.0511	−19.24	194.90	6.89	−18.27	0.97	−1206.0557	−16.73
Me																		
Keto-1	114.40				−642.3064		114.40				−642.3218		114.27				−642.3283	
Keto-2	114.33				−642.2964		114.27				−642.3156		114.27				−642.3239	
Dimer-1	230.80	6.80	−40.51	0.89	−1284.6551	−39.10	230.05	6.80	−27.02	0.89	−1284.6694	−23.88	229.92	6.79	−20.94	0.87	−1284.6751	−17.07
Enol	114.65				−642.3083		114.27				−642.3186		114.14				−642.3220	1.23
Dimer-2	230.48	6.97	−25.10	0.92	−1284.6557	−24.60	229.73	6.96	−20.03	0.92	−1284.6670	−18.77	229.42	6.95	−18.15	0.92	−1284.6706	−16.71
Pr																		
Keto-1	150.48				−720.9004		150.44				−720.9148		150.16				−720.9216	
Keto-2	150.41				−720.8904		150.46				−720.9092		150.35				−720.9177	
Dimer-1	303.02	6.84	−40.66	0.89	−1441.8433	−39.29	302.40	6.82	−27.06	0.88	−1441.8568	−24.05	302.08	6.82	−21.04	0.87	−1441.8627	−17.16
Enol	150.73				−720.9021		150.35				−720.9116		150.10				−720.9163	0.95
Dimer-2	302.71	6.95	−24.51	0.93	−1441.8430	−24.32	301.83	6.96	−20.02	0.93	−1441.8531	−18.73	301.52	6.96	−18.02	0.93	−1441.8590	−16.61
iPr																		
Keto-1	150.29				−720.8994		150.16				−720.9138		150.04				−720.9204	
Keto-2	150.23				−720.8894		150.29				−720.9081		150.16				−720.9166	
Dimer-1	302.59	6.86	−40.83	0.91	−1441.8414	−39.29	302.15	6.83	−27.06	0.88	−1441.8546	−24.03	301.77	6.82	−21.10	0.87	−1441.8605	−17.19
Enol	150.48				−720.9014		150.10				−720.9111		149.91				−720.9151	0.95
Dimer-2	302.27	6.99	−24.51	0.94	−1441.8416	−24.30	301.33	6.98	−20.01	0.94	−1441.8520	−18.69	300.95	6.97	−18.00	0.93	−1441.8568	−16.67
Ad																		
Keto-1	238.08				−992.4067		237.89				−992.4210		237.64				−992.4277	
Keto-2	238.14				−992.3969		238.08				−992.4158		237.95				−992.4242	
Dimer-1	478.29	6.86	−40.95	0.89	−1984.8570	−39.66	477.60	6.87	−27.27	0.90	−1984.8703	−24.31	477.10	6.86	−21.12	0.90	−1984.8762	−17.37
Enol	238.39				−992.4087		237.89				−992.4184		237.70				−992.4225	0.93
Dimer-2	477.91	6.99	−24.51	0.93	−1984.8561	−24.30	476.97	6.99	−19.80	0.92	−1984.8664	−18.55	476.53	6.99	−17.99	0.92	−1984.8713	−16.59

^a^bE values are in the unit of au, and others are in kcal/mol. Superscripts a and b represent the results at the B3LYP/6-311+G(2d,2p) levels. Energies (E) and binding energies (E_b) in the table are corrected by ZPE and BSSE corrections.

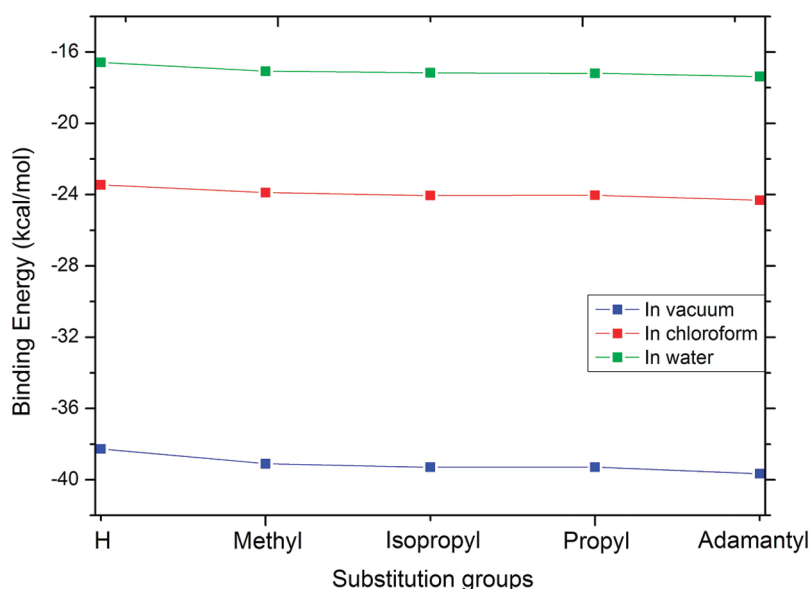


Figure 2. Binding energies in *Dimer-1* in various environments.

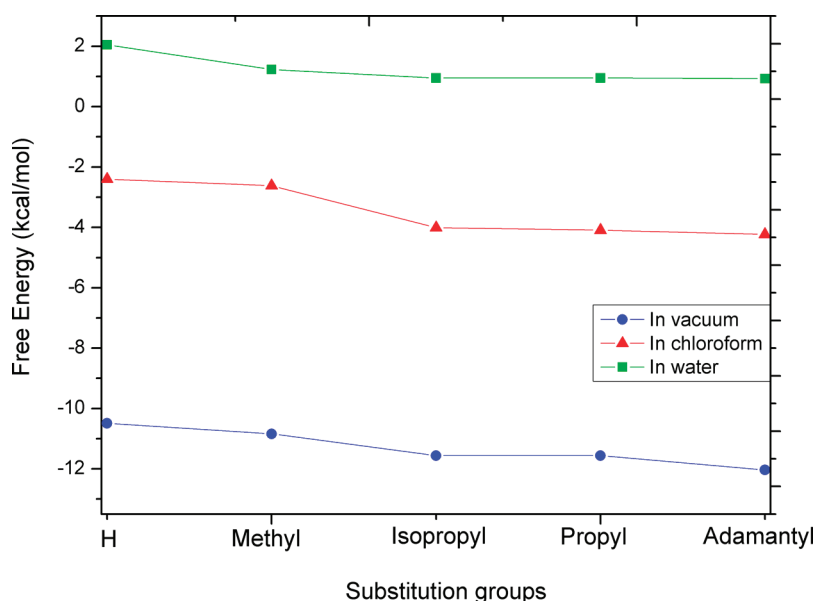


Figure 3. Free energies in *Dimer-1* in various environments.

more profound understanding of dimerization, the free energies of dimerization of UPy-6-Me *Dimer-1* were calculated. It should be remembered that the most stable forms of monomers are *Keto-1* in solvent and *Enol* in a vacuum, respectively. Therefore, the free energy of dimerization should be the difference of standard free energy of *Dimer-1* and the most stable monomers but not *Keto-2*.³⁴ That is,

$$\Delta G = G_{dimer-1}^0 - 2G_{Enol}^0 \quad (\text{in a vacuum}) \quad (2)$$

$$\Delta G = G_{dimer-1}^0 - 2G_{ketol-1}^0 \quad (\text{in chloroform and water}) \quad (3)$$

From Table 2 and Figure 3, it can be seen that the free energies of dimerization in chloroform are negative, whereas those in water are

small positive values, which indicates the feasibility of dimerization in chloroform and the possibility in water. In addition, the free energies of dimerization increase with the increasing size of the substituents in both solvents, which also indicates that dimerization is promoted when the substituent has a stronger electron-donating ability.

Effect of Explicit Solvent Surrounded by a Continuum Solvent. To provide more evidence of the feasibility of dimerization in chloroform and water, the explicit solvent surrounded by a continuum solvent, called the implicit–explicit model herein, was used to investigate the interaction between *Keto-2* form of UPy-6-Me and water molecules. Different from the traditional implicit solvent model, the implicit–explicit solvent model means solutes combined with varying numbers of explicit solvent molecules are treated as a supermolecule in continuum solvent.

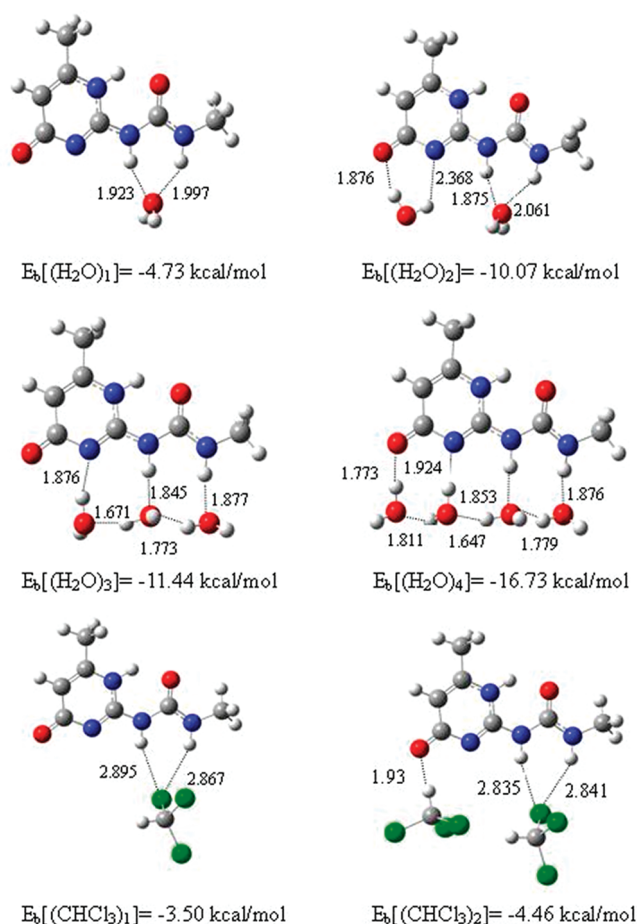


Figure 4. Optimized geometries of complexes of UPy-Me interacting with solvent molecules (unit: Å).

With the implicit–explicit model, one can get more comprehensive understanding of the coupling between solute and solvent molecules. The implicit–explicit model has been proved to give more accurate predictions of the solvent effect for complicated systems.^{53–55} Different numbers ($n = 1–4$) of solvent molecules were added manually around the *Keto-2* form of UPy-6-Me, and then the resulting complexes were optimized with PCM at the B3LYP/6-31G(d) level. Single point energies were calculated at the B3LYP/6-311++G(2d,2p) level. The most stable structures of clusters of UPy-6-Me, each with the corresponding number of solvent molecules, are shown in Figure 4. The energy values shown in Figure 4 have been corrected by ZPE and BSSE. The interaction energies were calculated according to $E_b = E(\text{complex}) - E(\text{UPy-6-Me}) - E(\text{solvents})$, where $E(\text{solvents})$ is the single point energy based on the structure in the corresponding complex. Figure 4 indicates that the binding energies increased with the increasing number of solvent molecules added around the UPy-6-Me molecule. The binding energies between UPy-6-Me and one and two CHCl_3 molecules are $E_b[(\text{CHCl}_3)_1] = -3.50$ kcal/mol and $E_b[(\text{CHCl}_3)_2] = -4.46$ kcal/mol, respectively, which is less competitive than the interaction between the two UPy-6-Me monomers in the *Dimer-1* (-23.88 kcal/mol) in chloroform. Therefore, it is not the interaction between UPy-6-Me and CHCl_3 molecules, but the dimerization that plays a much more important role in the mixture of UPy-6-Me and chloroform. However, the interaction between UPy-6-Me and

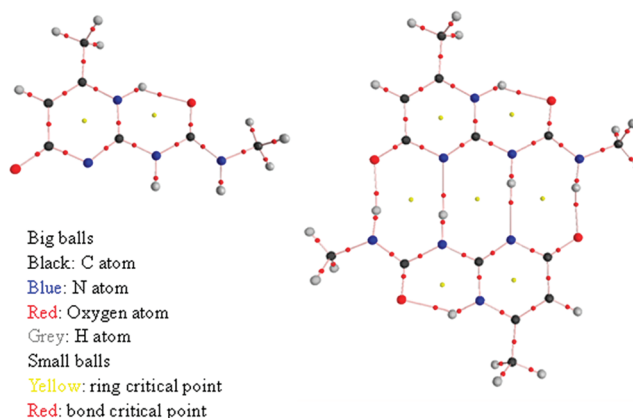


Figure 5. Molecular graph of UPy-Me monomer (*Keto-2*) and dimer (*Dimer-1*) at the B3LYP/6-311++G(2d,2p) level.

water molecules $E_b[(\text{H}_2\text{O})_n] = -4.73, -10.07, -11.44$, and -16.73 kcal/mol for $n = 1, 2, 3$, and 4 , respectively. $E_b[(\text{H}_2\text{O})_4]$ is comparable to the binding energy of *Dimer-1* (-17.07 kcal/mol) in water, indicating that the interaction between UPy-6-Me and water molecules is competitive with dimerization. Therefore, water molecules tend to disturb and damage the dimerization of UPy-6-Me.

Hydrogen Bonding Analysis. *Topology Analysis.* The theory of atoms in molecules (AIM) proposed by Bader⁴⁹ reveals the topology of electron density and further extrapolates molecular properties. Eight criteria were proposed by Popelier^{56–58} to characterize weak interactions such as hydrogen bonding, i.e., (1) appropriate topological patterns, especially there exists a bond critical point (BCP or $(3, -1)$ critical point) with $\lambda_1 \leq \lambda_2 < 0 < \lambda_3$ between H atoms and hydrogen bonding acceptor atoms (HBAA); (2) proper range of electron densities $\rho(r)$, of the BCP; (3) proper range of the Laplacian $\nabla^2\rho(r)$ ($\lambda_1 + \lambda_2 + \lambda_3$) of the electron density of BCP; (4) mutual penetration of H atoms and HBAA; (5) increased net charge of H atoms; (6) energetic destabilization of H atoms; (7) decrease of dipolar polarization of H atoms; (8) decrease of H atoms volume. Among these eight elements, Lipkowski⁶⁰ pointed out that the first three are most usually used for evaluating hydrogen bonding, and electron density $\rho(r)$ and the Laplacian $\nabla^2\rho(r)$ are in $0.002–0.04$ au and $0.002–0.015$ au, respectively. Figure 5 depicts a molecular graph with critical bond points of the UPy-6-Me dimer, whose structure was obtained by optimization in a vacuum. Table 3 gives the topology analysis of critical bond points for UPy-6-Me dimer in chloroform. Figure 5 and Table 3 show that bond critical points (BCP) $(3, -1)$ are found in two sets of $\text{N}(1)–\text{H}(1)–\text{O}(1)$, $\text{N}(2)–\text{H}(2)–\text{N}'(2)$, and $\text{N}(3)–\text{H}(3)–\text{O}(3)$, indicating the existence of hydrogen bonds between H and N or O atoms. Therefore, intramolecular and intermolecular hydrogen bonds coexist in the dimer. Topological analysis also shows that the electron densities $\rho(r)$ and its Laplacians $\nabla^2\rho(r)$ of BCP are in the proper range for hydrogen bonding proposed by Lipkowski.⁶⁰ All the values of λ_3 are much larger than λ_1 and λ_2 , which is a characteristic of close-shell interaction.

To evaluate the penetration between A atoms and H atoms, $\delta r = \Delta r_H + \Delta r_Y$ has also been calculated, where Δr is the non-bonded radius minus the bonded radius, i.e., $\Delta r = r_b(\text{in dimer}) - r_0(\text{in monomer})$. r_0 is defined as the distance of atomic nucleus to a given electron density contour in the monomer. As suggested by Popelier,⁵⁷ the value of 0.001 au is taken for the contour in the

Table 3. Topology Analysis of Critical Bond Points for UPy-6-Me Monomer (*Keto-2*) and Dimer (*Dimer-1*) at the B3LYP/6-311++G(2d,2p) Level^a

	BCP					H atoms							H...Y	
	$\rho(r)_1$	$\nabla^2\rho(r)_1$	λ_1	λ_2	λ_3	V	ΔV	q_H	δq_H	M	δM	E	δE	δr
<i>Keto-2</i>	N(1)–H(1)–O(1)	0.0328	0.1161	–0.0450	–0.0440	0.2050	21.08	0.4700		0.1317		–0.4332		
	N(2)–H(2)–O(2)						31.35	0.3677		0.1700		–0.4881		
	N(3)–H(3)–N(3)						29.57	0.4044		0.1641		–0.4663		
<i>Dimer-I</i>	N(1)–H(1)–O(1)	0.0408	0.1387	–0.0693	–0.0686	0.2766	18.57	0.4971	0.0271	0.1199	–0.0118	–0.4212	0.0118	–0.6156
	N(2)–H(2)–O(2)	0.0396	0.1118	–0.0626	–0.0607	0.2351	17.12	0.4841	0.1164	0.1111	–0.0588	–0.4278	0.0603	–1.1422
	N(3)–H(3)–N(3)	0.0291	0.0700	–0.0401	–0.0382	0.1483	19.22	–10.35	0.4716	0.0671	–0.0389	–0.4263	0.0040	–1.0944

† Structures of monomer and dimer were obtained from the optimization under vacuum condition.

^a Structures of monomer and dimer were obtained from the optimization under vacuum condition.Table 4. NBO Analysis of UPy-6-Me Monomer (*Keto-2*) and Dimer (*Dimer-1*) at the B3LYP/6-311++G(2d,2p) Level^a

	$q(N)$	$\delta q(N)$	$q(H)$	$\delta q(H)$	$\delta q_1(HAA)$	$s(N)$	$\delta s(N)$	$n\{LP_1(HAA)\}$	$\delta n\{LP(HAA)\}$	$\sigma^*(HDB)$	$\delta \sigma^*(HDB)$	$E\{LP_{(HAA)} - \sigma^*(N-H)\}$	
<i>Keto-2</i>													
<i>Dimer-1</i>													

^a Structures of the monomer and dimer were obtained from the optimization under vacuum conditions. HAA and HDB represent H-bond acceptor atom and H-bond donor bond, respectively.

computations. r_b is the distance from the nucleus to the BCP in the dimer. The negative δr demonstrates that mutual penetration occurs between H atoms and A atoms. Furthermore, intra- and intermolecular hydrogen bonds are formed in these dimers. When hydrogen bonds are formed, the electrons transfer from the H atoms to the A atoms resulted in a difference of the overall net charges of these H atoms to range from 0.0271 to 0.1164 au. As a result of dimerization, energies of H atoms are enhanced, where an increment from 0.0118 to 0.0603 au was calculated. Dipolar polarizations and volume of H atoms both decreased after the monomers dimerize. All this evidence is consistent with the existence of quadruple hydrogen bonding in the dimer.

NBO Analysis. NBO analysis is another efficient tool to explain and evaluate the properties of hydrogen bonds. As proposed by Alabugin,⁵⁹ hydrogen bonds are the cocontribution and the simultaneous competition of hyperconjugation and rehybridization. Here, we also take the UPy-6-Me monomer and dimer as examples to get further understanding of the quadruple hydrogen bonds as well as intramolecular hydrogen bonds. Table 4 lists the hyperconjugation energies of interacting orbitals forming hydrogen bonds, variations of natural atomic charge of H atoms, occupancies of natural bond orbitals and s-characters of A atoms. Because O atoms have two asymmetric lone pairs of electron, there are two different values of hyperconjugation energies between its lone pairs of electron and antibonding orbitals the hydrogen-bond donator bond N–H. Hyperconjugative interactions for intramolecular hydrogen bonding increased when a dimer was formed. According to Alabugin's report,⁵⁹ the hyperconjugation energies of strong hydrogen bonds (over 11 kcal/mol) resulted in the elongation of the N–H bonds along with red-shifting. Similarly, the UPy-6-Me dimer also demonstrated such properties, which is supported by our geometric results and frequencies as listed in Table 1S (Supporting Information) and Table 1. Due to the hyperconjugation, electron is transferred from lone pairs (LP) of electron of O or N atoms to N–H bonds in all inter- or intramolecular hydrogen bondings. Therefore, occupancies of LPs of O or N atom decrease and those of antibonding N–H bonds increase at the same time. 3D images of donor and acceptor orbital interactions are shown in Figure 6.

The contribution of rehybridization can be interpreted by analyzing the s-character of hybrid orbitals of N atoms of N–H bonds involved in the hydrogen bonds. The s-character of N atoms in the three hydrogen bonds were found to increase as a result of rehybridization (Table 4). In principle, rehybridization contributes to strengthen N–H bonds and leads to shorter N–H bonds. In addition, positive charges on H(2) and H(3) atoms increase and the charges on N(2) and N(3) atoms become more negative from monomer to dimer. This can be considered to be a result of repolarization, which also may decrease the length of N–H bonds. For intramolecular hydrogen bonding N(1)–H(1)···O(1), however, the charge on H(1) becomes more positive whereas the charge on N(1) becomes less negative, and these two opposite repolarizations (positive and negative) compete with each other. Because the charges on all N and H atoms do not vary significantly, the repolarization can be neglected in the system.

From the above analysis, competitive effects that can lengthen or shorten N–H bonds coexist in three hydrogen bonds of the dimer. Interacting energies between HB acceptors and donor orbitals are much higher than 11 kcal/mol, whereas extents of repolarization and rehybridization are not significant. Therefore, hyperconjugation may play a dominant role in lengthening N–H bonds and causing a red shift to their stretching vibrational modes. N–H

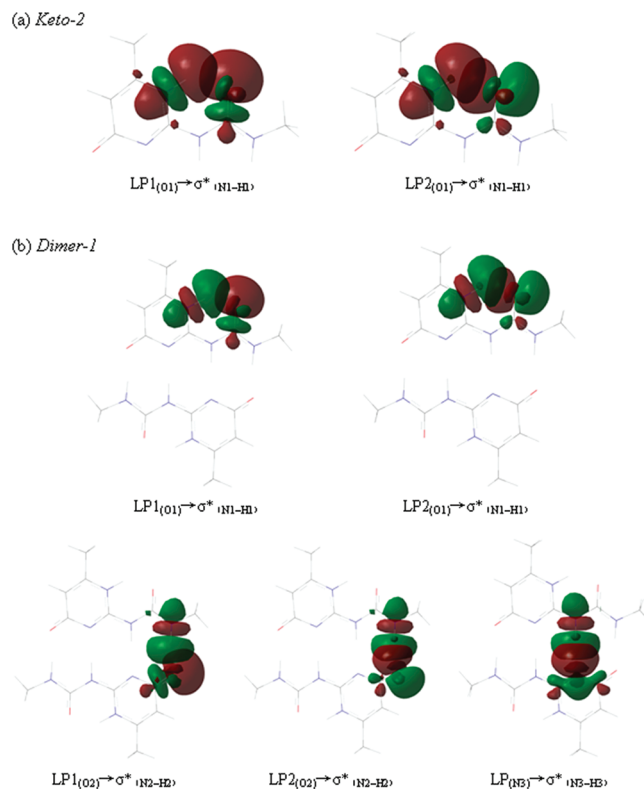


Figure 6. Visual 3D images of donor and acceptor orbital interaction of UPy-Me monomer (*Keto-2*) and dimer (*Dimer-1*) at the B3LYP/6-311++G(2d,2p) level.

bonds in intermolecular hydrogen bonds exhibit negative rehybridization, which contributes to larger bond lengths and red shift of N–H stretches. This result is also in good agreement with the geometry shown in Table 1S (Supporting Information) and IR values listed in Table 2.

CONCLUSIONS

A series of UPy-based monomers with various substituents at position 6 of the pyrimidinone ring and their corresponding dimers have been studied by DFT methods. The computations showed the possible existence of three monomers (*Keto-1*, *Keto-2*, and *Enol*) and two dimers under various experimental conditions (e.g., in a vacuum, chloroform, and water). The *Enol* monomer is found to be most stable in a vacuum, whereas the *Keto-1* monomer demonstrated the lowest energy in both chloroform and water. In the most investigated environments, *Dimer-1* is generally more stable than *Dimer-2*. Evidence of intramolecular and intermolecular hydrogen bonds in *Dimer-1* was found by topological analysis. Frequency and NBO calculations showed that these hydrogen bonds exhibit an obvious red shift in their stretching vibrational frequencies.

Two factors are found to contribute to the dimerization of *Keto-2* monomer of UPy derivatives. First, substituents with larger size and stronger electron-donating ability give rise to more stable *Dimer-1* and the possibility of dimerization both in a vacuum and in solvents. Second, the computations performed with both the implicit solvent model and the implicit–explicit solvent model showed that dimerization should not occur in water but is favored in weakly polar chloroform. Interaction of the water molecules with N–H of the pyrimidinone ring is

strongly competitive with the dimerization of *Keto*-2. Further structure modification may be effective in achieving a stable H-bonded network in water. Related experimental and theoretical work is currently performed in our laboratories.

■ ASSOCIATED CONTENT

S Supporting Information. Comparisons of geometric parameters obtained at the B3LYP/6-31G(d) level with available results at the B3LYP/6-311+G(d,p) level. Calculated bond distances for N(1)–H(1)---O(1)/N(1), N(2)/O(2)–H(2)---O(2), and N(3)–H(3)---N(3) bonds in all monomers and dimers. This material is available free of charge via the Internet at <http://pubs.acs.org>.

■ AUTHOR INFORMATION

Corresponding Author

*E-mail: s.smith@uq.edu.au. Tel.: 61-7-3346-3949. Fax: 61-7-3346-3992.

■ ACKNOWLEDGMENT

We thank the reviewers for their comments. This research was undertaken in the National Computational Infrastructure (NCI) National Facility at the ANU and CCMS cluster computing facility at AIBN.

■ REFERENCES

- (1) Zimmerman, N.; Moore, J. S.; Zimmerman, S. C. *Chem. Ind.* **1998**, 604–610.
- (2) Moore, J. S. *Curr. Opin. Colloid Interface Sci.* **1999**, 4, 108–115.
- (3) Ciferri, A., Ed. *Supramolecular Polymers*; Marcel Dekker, Inc.: New York, 2000.
- (4) Zimmerman, S. C.; Corbin, P. S. *Struct. Bonding (Berlin)* **2000**, 96, 63–94.
- (5) Brunsveld, L.; Folmer, B. J. B.; Meijer, E. W.; Sijbesma, R. P. *Chem. Rev.* **2001**, 101, 4071–4098.
- (6) Sherrington, D. C.; Taskinen, K. A. *Chem. Soc. Rev.* **2001**, 30, 83–93.
- (7) Prins, L. J.; Reinhoudt, D. N.; Timmerman, P. *Angew. Chem., Int. Ed.* **2001**, 40, 2382–2426.
- (8) Armstrong, G.; Buggy, M. J. *Mater. Sci.* **2005**, 40, 547–551.
- (9) Binder, W. H.; Zirbs, R. *Adv. Polym. Sci.* **2007**, 207, 1–78.
- (10) ten Brinke, G.; Ruokolainen, J.; Ikkala, O. *Adv. Polym. Sci.* **2007**, 207, 113–177.
- (11) Wilson, A. J. *Soft Matter* **2007**, 3, 409–425.
- (12) Dankers, P. Y. W.; Meijer, E. W. *Bull. Chem. Soc. Jpn.* **2007**, 80, 2047–2073.
- (13) de Greef, T. F. A.; Meijer, E. W. *Nature* **2008**, 453, 171–173.
- (14) de Greef, T. F. A.; Smulders, M. M. J.; Wolfs, M.; Schenning, A. P. H. J.; Sijbesma, R. P.; Meijer, E. W. *Chem. Rev.* **2009**, 109, 5687–5754.
- (15) Fouquey, C.; Lehn, J.-M.; Levelut, A.-M. *Adv. Mater.* **1990**, 2, 254–257.
- (16) Kato, T.; Wilson, P. G.; Fujishima, A.; Fréchet, J. M. J. *Chem. Lett.* **1990**, 2003.
- (17) Wilson, A. J. *Nat. Chem.* **2011**, 3, 193–194.
- (18) Beijer, F. H.; Kooijman, H.; Spek, A. L.; Sijbesma, R. P.; Meijer, E. W. *Angew. Chem., Int. Ed.* **1998**, 37, 75–78.
- (19) Sijbesma, R. P.; Beijer, F. H.; Brunsveld, L.; Folmer, B. J. B.; Hirschberg, J. H. K. K.; Lange, R. F. M.; Lowe, J. K. L.; Meijer, E. W. *Science* **1997**, 278, 1601–1604.
- (20) Beijer, F. H.; Sijbesma, R. P.; Kooijman, H.; Spek, A. L.; Meijer, E. W. *J. Am. Chem. Soc.* **1998**, 120, 6761–6769.
- (21) Lange, R. F. M.; van Gurp, M.; Meijer, E. W. *J. Polym. Sci. A: Polym. Chem.* **1999**, 37, 3657–3670.
- (22) Lafitte, V. G. H.; Aliev, A. E.; Horton, P. N.; Hursthouse, M. B.; Bala, K.; Golding, P.; Hailes, H. C. *J. Am. Chem. Soc.* **2006**, 128, 6544–6545.
- (23) Greco, E.; Aliev, A. E.; Lafitte, V. G. H.; Bala, K.; Duncan, D.; Pilon, L.; Golding, P.; Hailes, H. C. *New J. Chem.* **2010**, 34, 2634–2642.
- (24) Park, T.; Zimmerman, S. C.; Nakashima, S. *J. Am. Chem. Soc.* **2005**, 127, 6520–6521.
- (25) Hisamatsu, Y.; Shirai, N.; Ikeda, S.; Odashima, K. *Org. Lett.* **2010**, 12, 1776–1779.
- (26) Brammer, S.; Lüning, U.; Kühl, C. *Eur. J. Org. Chem.* **2002**, 4054–4062.
- (27) Taubitz, J.; Lüning, U. *Aust. J. Chem.* **2009**, 62, 1550–1555.
- (28) Blight, B. A.; Hunter, C. A.; Leigh, D. A.; McNab, H.; Thomson, P. I. *T. Nat. Chem.* **2011**, 3, 244–248.
- (29) Jorgensen, W. L.; Pranata, J. *J. Am. Chem. Soc.* **1990**, 112, 2008–2010.
- (30) Söntjens, S. H. M.; Sijbesma, R. P.; van Genderen, M. H. P.; Meijer, E. W. *J. Am. Chem. Soc.* **2000**, 122, 7487–7493.
- (31) Folmer, B. J. B.; Sijbesma, R. P.; Versteegen, R. M.; van der Rijt, J. A. J.; Meijer, E. W. *Adv. Mater.* **2000**, 12, 874–878.
- (32) Sijbesma, R. P.; Meijer, E. W. *Chem. Commun.* **2003**, 5–16.
- (33) Keizer, H. M.; van Kessel, R.; Sijbesma, R. P.; Meijer, E. W. *Polymer* **2003**, 44, 5505–5511.
- (34) de Greef, T. F. A.; Nieuwenhuizen, M. M. L.; Sijbesma, R. P.; Meijer, E. W. *J. Org. Chem.* **2010**, 75, 598–610.
- (35) Nieuwenhuizen, M. M. L.; de Greef, T. F. A.; van der Bruggen, R. L. J.; Paulusse, J. M. J.; Appel, W. P. J.; Smulders, M. M. J.; Sijbesma, R. P.; Meijer, E. W. *Chem.—Eur. J.* **2010**, 16, 1601–1612.
- (36) Stepanian, S. G.; Radchenko, E. D.; Sheina, G. G.; Blagoi, Yu. P. *J. Mol. Struct.* **1990**, 216, 77–90.
- (37) Bühlmann, P.; Simon, W. *Tetrahedron* **1993**, 35, 7627–7636.
- (38) Su, M. D.; Chu, S. Y. *J. Am. Chem. Soc.* **1999**, 121, 4229–4237.
- (39) Han, S. Y.; Oh, H. B. *Chem. Phys. Lett.* **2006**, 432, 269–274.
- (40) Dong, H.; Hua, W. J.; Li, S. H. *J. Phys. Chem. A* **2007**, 111, 2941–2945.
- (41) Iche-Tarrat, N.; Barthelat, J. C.; Vigroux, A. *J. Phys. Chem. B* **2008**, 112, 3217–3221.
- (42) Gomez, P. C.; Galvez, O.; Escibano, R. *Phys. Chem. Chem. Phys.* **2009**, 11, 9710–9719.
- (43) Tabatchnik, A.; Blot, V.; Pipelier, M.; Dubreuil, D.; Renault, E.; Questel, J. Y. L. *J. Phys. Chem. A* **2010**, 114, 6413–6422.
- (44) Becke, A. D. *Phys. Rev. A* **1988**, 38, 3098–3100.
- (45) Lee, C.; Yang, W.; Parr, R. G. *Phys. Rev. B* **1988**, 37, 785–788.
- (46) Miertus, S.; Scrocco, E.; Tomasi, J. *Chem. Phys.* **1981**, 55, 117–129.
- (47) Miertus, S.; Tomasi, J. *Chem. Phys.* **1982**, 65, 239–245.
- (48) Frisch, M. J.; Trucks, G. W.; Schlegel, H. B.; Scuseria, G. E.; Robb, M. A.; Cheeseman, J. R.; Scalmani, G.; Barone, V.; Mennucci, B.; Petersson, G. A.; et al. *Gaussian 09*, Revision A.02; Gaussian, Inc.: Wallingford, CT, 2009.
- (49) Bader, R. F. W. *Chem. Rev.* **1991**, 91, 893–928.
- (50) Boys, S. F.; Bernardi, F. *Mol. Phys.* **1970**, 19, 553–566.
- (51) Simon, S.; Duran, M.; Dannenberg, J. J. *J. Chem. Phys.* **1996**, 105, 11024–11031.
- (52) Jeffrey, G. A. *An Introduction to Hydrogen Bonding*; Oxford University Press: Oxford, U.K., 1997.
- (53) Alexandrova, A. N.; Jorgensen, W. L. *J. Phys. Chem. B* **2007**, 111, 720–730.
- (54) Precechtelova, J.; Munzarova, M. L.; Novak, P.; Sklenar, V. *J. Phys. Chem. B* **2007**, 111, 2658–2667.
- (55) Marenich, A. V.; Cramer, C. J.; Truhlar, D. G. *J. Chem. Theory Comput.* **2010**, 6, 2829–2844.
- (56) Koch, U.; Popelier, P. L. A. *J. Phys. Chem.* **1995**, 99, 9747–9754.
- (57) Popelier, P. L. A. *J. Phys. Chem. A* **1998**, 102, 1873–1878.
- (58) Popelier, P. *Atoms in Molecules. An Introduction*; Prentice Hall, Pearson Education Limited: New York, 2000.
- (59) Alabugin, I. V.; Manoharan, M.; Peabody, S.; Weinhold, F. *J. Am. Chem. Soc.* **2003**, 125, 5973–5987.
- (60) Lipkowsky, P.; Grabowski, S. J.; Robinson, T. L.; Leszczynski, J. *J. Phys. Chem. A* **2004**, 108, 10865–10872.